

## Polyphenol– $\beta$ -Casein Complexes at the Air/Water Interface and in Solution: Effects of Polyphenol Structure

V. AGUIÉ-BÉGHIN,<sup>\*,†</sup> P. SAUSSE,<sup>†</sup> E. MEUDEEC,<sup>‡</sup> V. CHEYNIER,<sup>‡</sup> AND R. DOUILLARD<sup>†</sup>

INRA UMR 614 Fractionnement des Agro-Ressources et Environnement (FARE) INRA/Université de Reims Champagne Ardennes, Centre de Recherche en Environnement et Agronomie, 2 Esplanade R. Garros, BP 224, F-51686 Reims, France, and INRA-UMR Sciences Pour l'Oenologie, 2 Place Viala, Montpellier, France

The interactions between proteins and plant polyphenols are responsible for astringency and haze formation in beverages and may participate in foam stabilization. The effect of phenolic compounds with different structures, namely, catechin (C), epicatechin (Ec), epigallocatechin (Egc), epicatechin gallate (EcG), and epigallocatechin gallate (EgcG), on the surface properties at the air/liquid interface of  $\beta$ -casein, chosen as model protein, were monitored by tensiometry and ellipsometry. The formation of complexes in the bulk phase was measured by electrospray ionization mass spectrometry (ESI-MS). Adsorption of polyphenols from pure solution was not observed. Surface pressure, surface concentration, and dilational modulus of the protein adsorption layer were greatly modified in the presence of galloylated flavanol monomers (EcG and EgcG) but not of lower molecular weight polyphenols (<306 g/mol). The formation of polyphenol–protein aggregates in the bulk, as evidenced by ESI-MS and light scattering experiments, was related to the slowdown of protein adsorption.

**KEYWORDS:** Adsorption kinetics; adsorption layer;  $\beta$ -casein; polyphenols; protein–polyphenol interactions; spectroscopic ellipsometry; drop tensiometer; electrospray ionization mass spectrometry (ESI-MS), air/liquid interface

### INTRODUCTION

Polyphenols ( $\phi$ ) are aromatic plant metabolites, which are found in leaves and fruits of higher plants and thus in many foods and beverages made from them. Polyphenols are well known to bind to proteins in solution and to form complexes whose properties depend on the structure of both the polyphenol and the protein (1–3). This complexation is responsible for the reduction of dietary protein digestibility and the inhibition of digestive enzymes (4). In the food industry, polyphenols are often involved in the formation of protein precipitates in beverages (5–8) and in organoleptic properties such as astringency that is due to the precipitation of salivary proteins (9–12). In spite of the numerous studies relating the nature of the polyphenol–protein interaction in solution, understanding of this process is still partial because of the great diversity of the structures of polyphenolic compounds and proteins.

These associations can be soluble or not and reversible or not (4). Among polyphenols, tannins, including condensed tannins that are oligomers and polymers of flavan-3-ol units

and hydrolyzable tannins that consist of a polyol central core acylated by a variable number of gallic or ellagic acid units, are well known to interact with proteins. Their efficacy as protein-complexing agents depends on their molecular size (13, 14) and oxidation state (15). It increases with the number of phenolic groups and associated aromatic rings the presence of several phenolic rings in a tannin molecule, enabling it to build bridges between the proteins (16) or with other polyphenols (17). In particular, acylation of the flavanol units with gallic acid, as encountered in tea and grape seed flavanols, increases flavanol affinity for proteins (18) and peptides (19) as well as their astringency perception (20). Moreover, it has been shown that proline rich proteins have a greater affinity for polyphenols than other proteins (17, 21, 22). This particular group of proteins, showing extended structure in solution and thus belonging to intrinsically unstructured proteins (23), include salivary proline rich proteins (PRP) that are responsible for astringency perception, prolamines that are involved in haze formation in beer, and finally gelatins and caseins that are used as fining agents to precipitate tannins from wine and other beverages (24). Since salivary PRP and gelatins are difficult to obtain in a pure state and the peptides used so far to mimic salivary proteins lack the ability to acquire secondary structure through interaction with tannins,  $\beta$ -casein was selected as a suitable model for these

\* Corresponding author. E-mail: Veronique.Aguie@reims.inra.fr.

<sup>†</sup> INRA-UMR Fractionnement des Agro-Ressources et Environnement (FARE) INRA/URCA.

<sup>‡</sup> INRA-UMR Sciences Pour l'Oenologie.

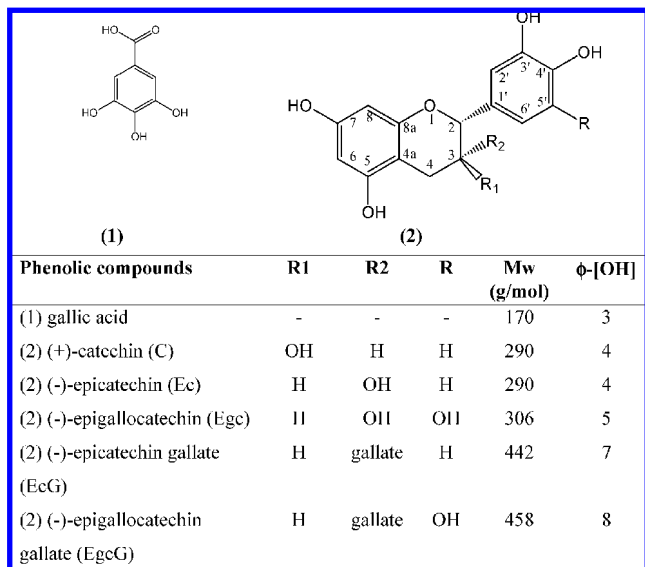


Figure 1. Structures of the phenolic compounds.

PRP because of its flexible random coil, low level of secondary structure ( $\sim 10\%$   $\alpha$ -helix and  $\sim 13\%$   $\beta$ -sheet), and high proportion of proline residues (16%) (25).

Studies in our laboratories were undertaken to check the effects of polyphenolic compounds on the structure and properties of adsorption layers formed at the gas/liquid interface and known to stabilize foams and emulsions. A special interest is focused on sparkling wines, which contain some phenolic compounds (26) and where the stability of the bubbles (or bubble collar) is clearly related to the formation of a macromolecule adsorption layer (27, 28). In a previous work, the effect of epigallocatechin gallate on  $\beta$ -casein adsorption was investigated by tensiometry and ellipsometry (29). Several effects were particularly striking: (i) an increase of the induction time of the protein adsorption kinetics related to the polyphenol bulk concentration, (ii) an increase of the protein surface concentration ( $\beta$ -casein) in the adsorption layer between 0 and 20 mg/L of polyphenol in the bulk, and (iii) an increase of the elastic modulus after the formation of the layer.

A series of flavanol monomers representative of common tannin constitutive units, namely, catechin (C), epicatechin (Ec), epigallocatechin (Egc), epicatechin gallate (EcG), and epigallocatechin gallate (EgcG) (Figure 1) were tested along with gallic acid, to complete this study and highlight the effect of major characteristic features of tannin structure: configuration of carbon C3 (C compared to Ec), presence of *o*-diphenol or triphenol groups (gallic acid, Ec compared to Egc, EcG compared to EgcG), and galloylation (Ec and Egc compared to EcG and EgcG).

In the present study, to check the mechanism of formation of the adsorption layer, a comparison was made of the interactions between  $\beta$ -casein and phenolics in the adsorption layer and in the bulk. In the bulk, electrospray ionization mass spectrometry (ESI-MS) measurements were performed since this approach reveals molecular interactions driven by noncovalent forces (30). The electrospray process is a soft ionization technique that allows the transfer of noncovalent complexes (hydrogen bonds and hydrophobic interactions) (31, 32) into the mass analyzer and has been successfully applied to study polyphenol/peptide complexes (19, 33). Thus, relative affinities between protein and phenolic compounds were observed at the air/liquid interface and in solution. This allows one to cross-validate the methods and in particular to evaluate the relevance

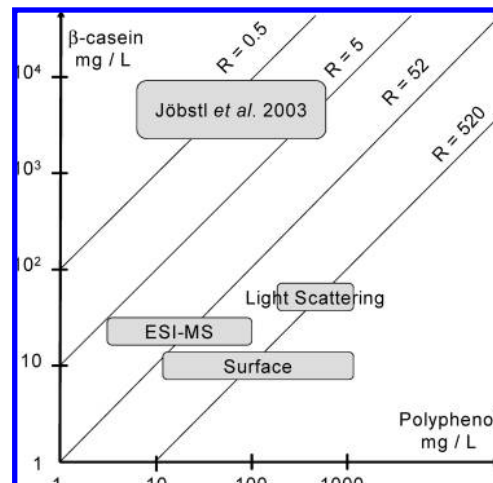


Figure 2. Concentrations of polyphenol ( $\phi$ ) and of  $\beta$ -casein used for surface and bulk experiments.  $R = \phi/\beta$ -casein (mol/mol).

of the ESI-MS and surface property measurement approaches to study tannin–protein interactions.

## MATERIALS AND METHODS

**Materials.**  $\beta$ -Casein was purified according to the method of Mercier et al. (34). Acid casein was prepared from the skimmed milk of a single cow homozygous for the three major caseins ( $\alpha$ s1B,  $\beta$ B, and  $\kappa$ B) and freeze-dried. Acid casein was then fractionated by ion exchange chromatography on DEAE 5PW using a NaCl gradient in a 20 mM imidazole buffer (pH 7), 3.3 M urea, and 1 mM DTT (dithiothreitol). The fraction corresponding to  $\beta$ -casein was rechromatographed in the same conditions, and its purity checked by polyacrylamide gel electrophoresis. The extinction coefficient used to determine the  $\beta$ -casein concentration in solution is  $\epsilon^{1\%}_{1\text{ cm}} = 4.6$  with a molecular mass of 24089 g/mol at 280 nm. EgcG (purity >95%), EcG (purity >98%), Egc (purity >98%), Ec (purity >98%), and C (purity >98%) were obtained from Sigma products (Sigma Chemical, Poole, Dorset, UK), and gallic acid (purity 99%) was obtained from Merck (KgaA, Darmstadt, Germany).

Each phenolic compound was ultrafiltered with a cutoff of 10,000 to remove amphiphilic macromolecular impurities from the samples.

**Sample Preparation.** Protein and protein–polyphenol mixtures were prepared in a 10 mM MOPS (morpholinopropane sulfonic acid) buffer, pH 7, for surface property experiments and in 10 mM ammonium acetate buffer, pH 7, for ESI-MS measurements according to ref 19. The protein bulk concentration was adapted according to the sensitivity of each method and was fixed to 10 mg/L (0.41  $\mu$ M) in all surface property measurements, to 28.3 mg/L (1.17  $\mu$ M) in ESI-MS measurements, and to 50.8 mg/L (2.1  $\mu$ M) in dynamic light scattering measurements. Polyphenol solutions were prepared just before use in order to avoid oxidation. Polyphenol solutions were prepared as 1 g/L stock solutions and added to  $\beta$ -casein solutions giving  $\phi/\beta$ -casein molar ratio ranges, respectively, from 0 to 7000, from 20 to 128 and from 0 to 520 in all surface, ESI-MS, and dynamic light scattering measurements (Figure 2). All samples were poured into glass vessels that were treated with chromosulfuric acid and rinsed with ultrapure water.

**Dynamic Bubble Tensiometer.** For measurements of static and dynamic surface tension, a bubble tensiometer (IT Concept, Longesaigne, France) was used (35–37). The surface tension was measured through shape analysis of an air bubble formed at the tip of a stainless steel needle dipped in the solution. The needle is attached to a syringe whose plunger is precisely controlled by a micrometer screw driven by an electric motor. The bubble is illuminated with a beam of parallel light. The image is recorded by a CCD camera and is digitized to allow the analysis of its shape. The interfacial tension  $\gamma$  is determined by analyzing the profile of the bubble according to the Laplace equation (37). The surface pressure,  $\pi$  is the difference between the surface tension of the pure solvent  $\gamma_0$  and that of the solution with surface active molecules  $\gamma$ . All measurements were done at  $20 \pm 1$  °C. The

surface dilational modulus,  $\varepsilon$ , is defined as the ratio between the variation of surface tension,  $d\gamma$ , and the relative change in the surface area,  $dA/A = d\ln(A)$  (38):

$$\varepsilon = d\gamma/d \ln A = -d\pi/d \ln A \quad (1)$$

It was determined during sinusoidal fluctuations of the area of the bubble at a chosen amplitude ( $\varepsilon$  was independent of the relative variation of the area  $\Delta A/A$  when it was less than 15% of the mean area (39) at a frequency of 0.1 Hz). The area and the surface tension were calculated twice per second. A Fourier transform of the data was performed and only the first harmonic was retained.

The surface dilational modulus is a complex quantity ( $\varepsilon = \varepsilon' + i\varepsilon''$ ) with a storage part (elastic),  $\varepsilon'$ , and a loss part (viscous),  $\varepsilon''$  (40). When the behavior of the adsorption layer is purely elastic, no phase difference occurs between  $d\gamma$  and  $dA$ ; the viscous component can be neglected. On the contrary, when the relaxation process affects  $d\gamma$  during the periodical deformations of the area of the bubble, both parts of the dilational modulus (real and imaginary) depend to the phase angle,  $\delta$ , and the maxima variations of the surface tension,  $\Delta\gamma$  and of the area,  $\Delta A$ :

$$\varepsilon' = |\varepsilon| \cos \delta \text{ and } \varepsilon'' = |\varepsilon| \sin \delta \quad (2)$$

where  $|\varepsilon| = \Delta\gamma/(\Delta A/A)$ .

**Ellipsometry.** The samples were poured into a glass Petri dish (60 mm diameter) just before data acquisition in order to reduce oxidation. All of the measurements (kinetics) were done using a spectroscopic phase modulated ellipsometer (UVISEL, Jobin Yvon, Longjumeau, France) as described previously (29, 41). The spectroscopic measurements were monitored between 250 and 810 nm. The incident angle was set at 53.4°. All measurements were done in an air-conditioned room at  $20 \pm 1$  °C. The two ellipsometric angles  $\Psi$  and  $\Delta$  are linked to the reflectivity coefficients  $r_p$  and  $r_s$  of the incident polarized light reflected in the directions parallel and perpendicular to the incidence plane, respectively:

$$r_p/r_s = \tan \psi e^{i\Delta} \quad (3)$$

The kinetics measurements were performed at a fixed wavelength,  $\lambda$ , which corresponds to the Brewster conditions of the solvent defined by  $\Delta = \pm \pi/2$ . The ellipticity coefficient measured in the Brewster conditions for the substrate,  $\bar{\rho}_B$ , is defined by

$$\bar{\rho}_B = \tan \psi \sin \Delta \quad (4)$$

In the ideal case of an interface between two transparent media without roughness (Fresnel interface),  $\bar{\rho}_B$  is zero. In the case of thin layers for which the thickness  $h$  is much lower than the wavelength  $\lambda$ , Brewster angle ellipticity, given by the Drude equation (42), is proportional to the layer thickness,  $h$ , and increases as the difference between the refractive index of the layer,  $n_1$ , and the refractive index of the substrate,  $n_2$ , when an adsorption layer begins to form at the air/liquid interface, according to eq 5.

$$\bar{\rho}_B \propto h[n_1^2 - 1][n_1^2 - n_2^2]/n_1^2 \quad (5)$$

To obtain protein and polyphenol surface concentrations, thickness and refractive indexes of the layers have been determined from ellipsometric spectra by assuming a density profile as one homogeneous layer model. The complex refractive index of the substrate,  $N_2 = n_2 + ik_2$ , was obtained from a pure buffer spectrum in the wavelength range by analytical inversion of the Fresnel equations (43). A point per point numerical resolution was applied on ellipsometric spectra of layers formed from protein and polyphenol mixtures to obtain the refractive index,  $n_1$ , and the extinction coefficient,  $k_1$ , of the interfacial layer as a function of the wavelength, using the thickness determined by analytical resolution of the Fresnel equations in the visible wavelength range where protein and polyphenol do not absorb light. The polyphenol surface concentration was deduced from the relationship between the imaginary part of the refractive index of the layer,  $k$ , and the bulk extinction coefficient of the polyphenol at 280 nm,  $\varepsilon_{280}$ , as described in previous studies (29, 44). The  $\varepsilon_{280}$  of EgcG, EcG, and Egc were kept to 25.6, 30, and 3.5 L g<sup>-1</sup> cm<sup>-1</sup>, respectively. The refractive index increment of  $\beta$ -casein and of polyphenol (for the calculation of the de

Freijer formula (45)) are 0.18 cm<sup>3</sup> g<sup>-1</sup> and 0.19 cm<sup>3</sup> g<sup>-1</sup>, respectively, as previously used (29, 46).

**ESI-MS Analysis.** Mass spectra were measured on an LCQ Advantage instrument (ThermoFinnigan, San Jose, CA) equipped with an electrospray ionization source and an ion-trap analyzer (ESI-IT-MS). The polyphenol solution and  $\beta$ -casein/polyphenol mixtures were prepared immediately before analysis to avoid oxidation, unless otherwise specified. Each solution was injected into the mass spectrometer by means of a syringe infusion pump (250  $\mu$ L) with a flow rate of 2.5  $\mu$ L/min. The spectra were recorded in the positive ion mode, over the range 300–2000. The source voltage was set at 5600 V, the capillary voltage at 26 V, the capillary temperature at 200 °C, the sheath gas flow at the 50 index, and the auxiliary gas at 0.

**Dynamic Light Scattering.** The dynamic light scattering (DLS) measurements were carried out using the technique known as correlation of intensity. The experimental setup is equipped with a light source (Argon laser) of wavelength  $\lambda = 514$  nm, a BI-200SM goniometer, and a Brookhaven correlator (BI2030AT). The time-dependence of the scattered light was monitored at an angle of 90° from the incident beam. The normalized time autocorrelation of the scattered electric field  $g_1(t)$  was extracted from the autocorrelation functions of the intensity  $G_2(t)$  of the particles:

$$G_2(t) = \langle I(0)I(t) \rangle = A + Bg_1^2(t) \quad (6)$$

where  $A$  and  $B$  are constants. In the case of monodisperse particles, the function  $g_1(t)$  is an exponential function:

$$g_1(t) = e^{-\Gamma t} \quad (7)$$

where  $\Gamma$ , is the decay rate. If the samples are very dilute, the interactions are negligible, and the hydrodynamic radii of particles  $R_h$  are deduced from  $D$  by use of the Stokes–Einstein law:

$$R_h = kT/6\eta D \quad (8)$$

where  $k$  is the Boltzmann constant,  $T$  the temperature (25 °C),  $\eta$  the viscosity of the buffer ( $\eta = 0.8904$  cp), and  $D$  the diffusion coefficient deduced from  $\Gamma$  ( $D = \Gamma/q^2$  with  $q = (4\pi n/\lambda) \sin(\theta/2)$  and  $n$ , the refractive index of the solution). In practice, the functions  $g_1(t)$  were analyzed by using the cumulant method (47) in order to obtain a mean decay rate and to deduce the mean hydrodynamic radii of particles.

## RESULTS

In this section, the effects of polyphenol structure (**Figure 1**) are analyzed first on the formation of complexes in the adsorption layer and then in the bulk under suitable experimental conditions (**Figure 2**). A particular attention is also devoted to the oxidation, which may influence the formation and the structure of the complexes. The mechanisms of formation of the complexes are discussed. Finally, we highlight the consistency between the bulk and the surface characterization of the  $\phi$ / $\beta$ -casein complex formation.

**Complex Formation at the Air/Water Interface.** *Adsorption of Pure Components.* For pure polyphenol solutions (100 mg/L), after 24 h, the surface pressure was lower than 0.5 mN/m, and the ellipticity remained slightly negative like that of the buffer. On the contrary, protein adsorption at 10 mg/L exhibited typical kinetics with three phases: the induction time, the increasing surface pressure period, and the plateau region where the surface pressure is nearly constant (**Figure 3**), as previously observed (29). The comparison between the adsorption of the phenolic compounds and that of  $\beta$ -casein enables one to neglect the former in the frame of this work.

*Influence of Phenolic Compounds on  $\beta$ -Casein Adsorption Kinetics.* The effect of each phenolic compound on the kinetics of  $\beta$ -casein (10 mg/L) adsorption was quantified by the calculation of the ratio of effective ( $C_{\text{eff}}$ ) to total ( $C_{\text{tot}}$ )  $\beta$ -casein concentration (29). The effective concentration was deduced

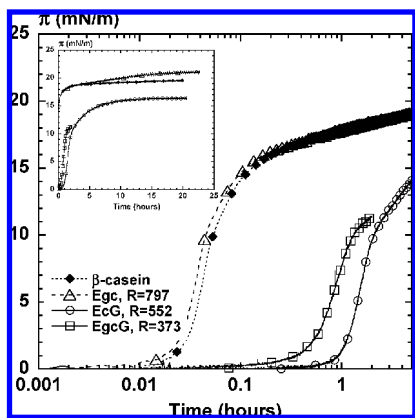


**Figure 3.** Effect of  $\beta$ -casein and polyphenol bulk concentrations on the induction time of the surface pressure kinetics with logarithmic scales. Adsorption layers were formed from  $\beta$ -casein (10 mg/L in 10 mM Mops buffer, pH 7) and its mixtures with EgcG, EcG, and Egc. The insert shows the total kinetics. The surface pressure was calculated twice per second.

from the mixture induction time and from the calibration curve of the induction time versus  $\beta$ -casein concentration. Its definition implies that the ratio  $C_{\text{eff}}/C_{\text{tot}}$  is equal to or smaller than one and that it decreases when the induction time increases. From a molar ratio ( $\phi/\beta$ -cas) of 150 of EgcG and EcG (about 30 mg/L  $\phi$ ), the ratio  $C_{\text{eff}}/C_{\text{tot}}$  quickly decreases (**Figure 4a**). For a molar ratio of 500 (or 90 mg/L) of EgcG and EcG, the effective protein concentration is less than 10% of the total protein. It can be concluded that the effects of EgcG and EcG on the  $\beta$ -casein adsorption are rather similar. Nevertheless, a small shift to lower concentrations is observed for EcG. Moreover, these mixed systems not only show an increase of the induction time but also a final surface pressure much lower than that obtained with pure  $\beta$ -casein (**Figure 3** insert). For a molar ratio ( $\phi/\beta$ -cas) of 213 for EgcG (40 mg/L, data not shown) and of 552 for EcG (100 mg/L), the surface pressure obtained after 24 h of protein adsorption at constant interfacial area is about 15 mN/m for both systems instead of 19 mN/m with the same bulk concentration of pure  $\beta$ -casein. Thus, in the presence of EgcG and EcG, the protein adsorption is significantly slower. On the contrary, the induction time and the final surface pressure are not altered by Egc, Ec, C, or gallic acid, even with high bulk concentrations of phenolic compounds ( $\geq 700$  mg/L) (**Figures 3** and **4b**). However, in the case of Egc at a molar ratio of 797 (100 mg/L), 6 h after the beginning of the adsorption, the surface pressure is 2 mN/m larger than in the case of pure  $\beta$ -casein solution (**Figure 3** insert) and in the case of Ec, C, or gallic acid in a mixture with  $\beta$ -casein. A likely hypothesis is that oxidation products of Egc are responsible of this last phenomenon (see next paragraph). Finally, surface pressure measurements indicate the formation of  $\beta$ -casein/polyphenol complexes in the case of EgcG, EcG, and Egc. For the first two molecules, these results are in agreement with other studies showing that galloylation of flavanol monomers strongly increases their interactions with proline rich proteins (48) and peptides (19). For the last one, the lag phase before the effect is measured suggests that the surface pressure is modified by oxidation products rather than Egc itself.

The questions are now of the mechanisms of the induction time increase with EgcG and EcG and of the delayed increase of the surface pressure with Egc. Several hypotheses about the induction time increasing can be put forward: modification of

the hydrophilic/hydrophobic balance of the protein chain, change of the conformation of the protein, or decrease of the diffusion coefficient.

**Modification of the Hydrophilic/Hydrophobic Balance.** Assuming that hydrophobic interactions between the protein and the polyphenol are involved in the formation of the complex, then the hydrophobicity of the complex should be less than that of the native protein. Thus, the increase of the induction time could be due to a loss of surface affinity of  $\beta$ -casein complexed with EgcG or EcG, a phenomenon increasing with bulk polyphenol concentration. Such interactions are expected especially in the case of galloylated molecules, which are reported to be rather hydrophobic (17, 49). However, a decrease of the induction time and consequently an increase of the hydrophobicity of the complex was not observed.

**Change of the Conformation of the Protein.** This hypothesis is supported by the work of Jöbstl et al. (50) showing that the radius of gyration of  $\beta$ -casein is reduced by its interaction with EgcG. The hydrophobic sites of the protein would be relatively buried by the conformation change leading to a situation looking like the previous one with a complex more soluble in water than the native  $\beta$ -casein.

**Decrease of the Diffusion Coefficient.** It has been shown previously that a decrease of the diffusion coefficient of a protein can induce an increase of the adsorption induction time (51). The corollary of this hypothesis is that the complexes occur as aggregates with a large hydrodynamic radius, which should be 50 times larger than that for pure  $\beta$ -casein from the very start of the adsorption kinetics (29). This point will be checked in the next paragraph by dynamic light scattering.

In the case of Egc, the delayed increase of the surface pressure is a strong argument for the presence of the polyphenol in the layer. However, since no increase of the induction time is observed, the mechanism of interaction is different from that of EgcG or EcG. Several hypotheses can be formulated.

**Affinity of Phenol for Protein.** The affinity of Egc for protein is significantly lower than that of EgcG or EcG since no increase of the induction time is noticed. This result is in agreement with the same ranking for EgcG, EcG, and Egc determined from partition coefficient measurements in octan-1-ol/water (48, 49). However, once the  $\beta$ -casein layer is formed, the concentration of protein in the surface layer is at least  $10^4$  times larger than that in the bulk, and the equilibrium of formation of a complex may be shifted toward the complex in that condition. Nevertheless, the kinetics of surface tension increase is delayed by several hours after layer formation. Thus, this hypothesis alone cannot explain the observed effect.

**Oxidation of Phenol.** The increase of surface pressure could be also related to the formation of a protein-oxidized polyphenol complex in the adsorption layer. After oxidation, the affinity of the phenol for  $\beta$ -casein is large enough for the formation of a complex as it has been observed in numerous situations. Then, the complexed polypeptide chain would have a more compact structure than the native protein, and its 2-D correlation length in the layer would decrease, inducing the surface pressure increase.

Whatever the mechanisms, the presence of the phenolic compounds and their possible oxidation in the adsorption layer should modify the properties of the layer, which are now studied by ellipsometry and by dilational rheology.

**Structure and Properties of the Adsorption Layer.** The total surface concentration as well as those of protein and of polyphenol in the adsorption layer were evaluated by ellipsometry. Indeed, the absolute value of Brewster ellipticity is

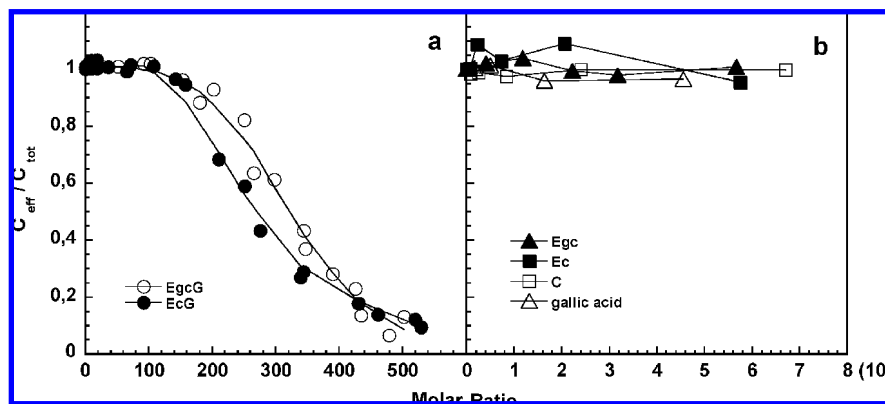


**Figure 4.** Effect of the bulk concentration of phenolic compounds on the adsorption kinetics of  $\beta$ -casein. Ratio of effective to total  $\beta$ -casein concentration (10 mg/L),  $C_{\text{eff}}/C_{\text{tot}}$ , versus molar ratio  $\phi/1/\beta$ -casein in the bulk. The effective casein concentration of a mixture is equal to the  $\beta$ -casein bulk concentration of a solution with the same induction time.

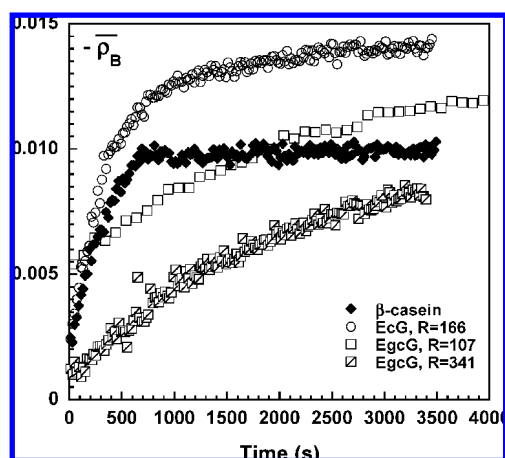


**Figure 5.** Effect of  $\beta$ -casein and polyphenol bulk concentrations on the kinetics of Brewster ellipticity. Adsorption layers were formed from  $\beta$ -casein (10 mg/L in 10 mM Mops buffer, pH 7) and its mixtures with EgCG and EcG. Kinetics of  $\beta$ -casein-Egc mixtures at molar ratios of 80 and 800 are identical to that of the protein alone during the first hour of adsorption.

practically proportional to the surface concentration of the adsorption layer, and spectroscopic ellipsometry also gives access to the absorption spectra of the molecules therein.

**Total Concentration of the Adsorption Layer.** For all studied polyphenols, in the adsorption experiments, ellipticity increased as soon as the sample was poured into the Petri dish, without any significant induction time, and reached a quasi-plateau (**Figure 5**) as previously observed for EgCG (29). For all polyphenols, the kinetics had the same pattern, and only the quasi-equilibrium situation is taken into account here. For EgCG and EcG, at equilibrium, the maximum ellipticity was 0.02 and 0.015, respectively, when the molar ratio  $\phi/1/\beta$ -casein varied between 50 and 250 (**Figure 6**) as compared to 0.011 for  $\beta$ -casein alone. Beyond a molar ratio of 250, the ellipticity decreased and became lower than that of pure  $\beta$ -casein. Egc for molar ratios between 100 and 800 also modified the ellipticity of the protein adsorption layer but with a response curve that is significantly different from that for EgCG and EcG. The ellipticity of the layer was around 0.02 for a molar ratio of 800. The other polyphenols tested had no significant effect in the whole concentration range explored.

These results on the global surface concentration of the layers show that EgCG and EcG behave similarly and interact strongly with the protein, inducing an increase of the surface concentration at low molar ratios and a depletion of the interfacial layer at high molar ratios. Egc also has a positive effect on the

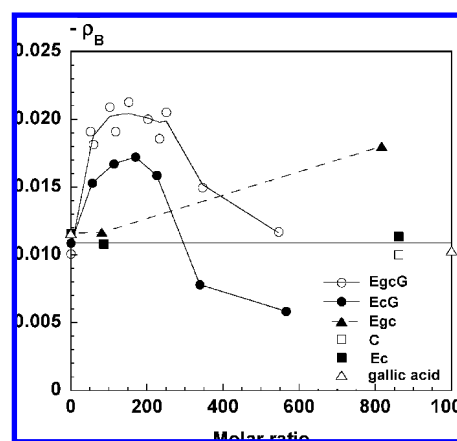


**Figure 6.** Effect of the bulk concentration of phenolic compounds on the Brewster ellipticity ( $-\rho_B$ ) at quasi-equilibrium state (24 h after the beginning of the adsorption). The concentration of  $\beta$ -casein is 10 mg/L in 10 mM Mops buffer, pH 7.

adsorption layer but only at a high concentration of polyphenol and without a noticed depletion effect.

**Concentration of the Components within the Adsorption Layer.** A further analysis of the ellipsometry spectra was conducted to evaluate the concentrations of the protein and of the phenolic compounds in the layer. Optical refractive and absorption indexes ( $n$  and  $k$ ) spectra of the layer were extracted from ellipsometric spectra for which Brewster ellipticity is high enough and close to 0.02, as described earlier (29). This extraction was possible when  $\beta$ -casein adsorbs from solution containing EgCG, EcG, and Egc (**Figures 7a** and **b**), but not when the polyphenol is Ec, C, or gallic acid since then the spectra are only representative of the refractive index (**Table 1**). The real index,  $n$ , is higher in the presence of EgCG, EcG, and Egc than for a pure  $\beta$ -casein adsorption layer (**Figure 7a**). Moreover, the spectrum of the imaginary part of the refractive index ( $k$ ) shows a maximum between 275 and 280 nm (**Figure 7b**). This absorption in UV could be allotted to the protein as well as to the polyphenol since these two molecules have an absorption maximum at 280 nm when they are in solution. Nevertheless, although the background noise does not allow accurate enough spectra to differentiate the origin of the UV absorption, no absorption was observed in the case of the layers formed from pure  $\beta$ -casein and from Ec, C, and gallic acid- $\beta$ -casein mixtures (**Figure 7b** and **Table 1**). This fact is certainly related to the values of the absorption coefficients ( $\epsilon_{280}$ ) since for  $\beta$ -casein in solution, it is roughly 50 times lower (0.46 L

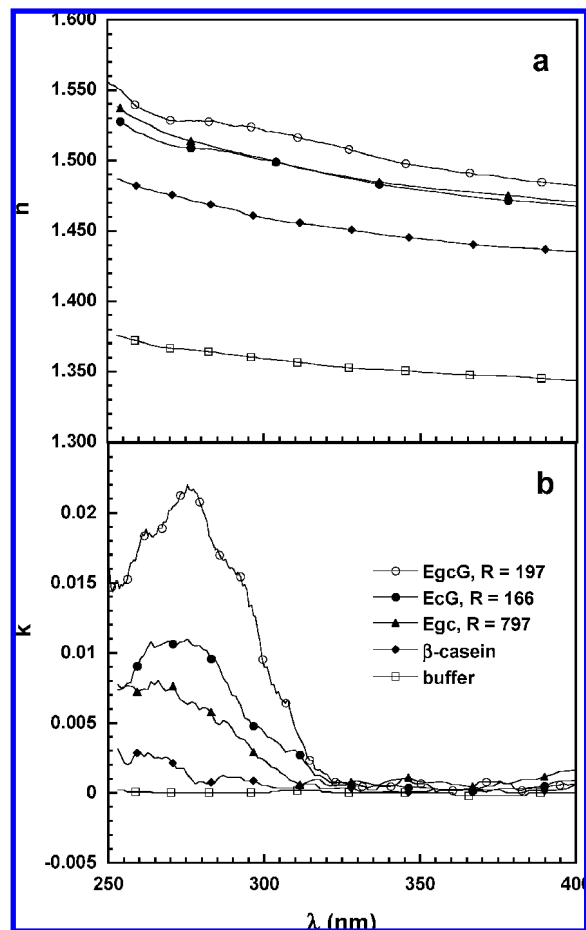


**Figure 7.** Real ( $n$ ) and imaginary ( $k$ ) parts of the refractive index of the layer formed from  $\beta$ -casein and polyphenol mixtures at various molar ratios  $\phi/\beta$ -casein ( $R$ ), 24 h after the beginning of adsorption.

$\text{g}^{-1} \text{cm}^{-1}$ ) than that for EgCG and EcG ( $\epsilon_{\text{EgCG}}$ ,  $25.6 \text{ L g}^{-1} \text{cm}^{-1}$ ;  $\epsilon_{\text{EcG}}$ ,  $30 \text{ L g}^{-1} \text{cm}^{-1}$ ) and 7 times lower than that for Egc ( $\epsilon_{\text{Egc}}$ ,  $3.5 \text{ L g}^{-1} \text{cm}^{-1}$ ). Thus, the optical absorption within the layer, whose thickness is of the order of 1 nm, is undoubtedly linked to the occurrence of polyphenols associated with  $\beta$ -casein. The surface concentrations of EgCG, EcG, and Egc within the adsorption layers were calculated (Table 1). After 24 h of adsorption, the polyphenol/protein molar ratio in the adsorption layer is  $15 \pm 3$ ,  $7 \pm 1$ , and  $85 \pm 25$  for EgCG, EcG, and Egc, respectively. The surface concentration of Egc is surprisingly much higher than that of the galloylated monomers. It should, however, be specified that the absorption spectrum of Egc in the layer is much less well defined than that of the two galloylated phenol complexes. Moreover, oxidation or polyphenol complex formation may significantly change the spectrum of Egc in the layer. Then, it is possible that the calculated surface concentration of Egc is not very accurate because of these effects (Table 1).

**Visco-Elastic Properties of the Adsorption Layer.** The visco-elastic properties of the adsorption layers formed from polyphenol and  $\beta$ -casein mixtures were approached by a dilational modulus and phase angle measurements to calculate the storage and loss moduli during 24 h after the beginning of the adsorption (eqs 1 and 2). This 24 h period was chosen to be in conditions where the delayed increase of surface pressure was observed with Egc. For EgCG or EcG, three molar ratios  $\phi/\beta$ -casein were chosen, corresponding to situations where, in the quasi-equilibrium state, the surface concentration increases, levels off, or

decreases as a function of the molar ratio (Figure 6). For Egc, similar molar ratios were used.

As a rule, the moduli increase slowly and may also decrease slowly during the time course of the experiment (kinetic not shown). There is no correlation between the moduli kinetics and the surface pressure and surface concentration kinetics.

With EgCG and EcG, the general trend is the same (Figure 8). The elastic component of the dilational modulus reaches a maximum for a molar ratio of the order of 200, where the surface concentration is the largest, and then decreases. In other words, when the adsorption is strongly reduced for large polyphenol concentrations in the bulk, the surface concentration decreases along with the surface pressure and the dilational modulus. There are, however, large differences between the values of the moduli or their kinetics when comparing EgCG and EcG. The elastic part of the modulus increases until 200 mN/m for EgCG and until 110 mN/m for EcG. This difference can be linked to the small shift of the ratio  $C_{\text{eff}}/C_{\text{tot}}$  observed for EcG (Figure 4) and to the significant difference of the surface concentration between EgCG and EcG (Figure 6). At this point of the results, it is worth stressing that these differences between the two galloylated  $\phi$ s are related to the presence of an additional hydroxyl group in C5' in the EgCG structure, which confers EgCG increased hydrophilicity and lower oxido-reduction potential (52, 53). For Egc with a bulk molar ratio range between 0 and 800, an increase of the elastic part of the modulus from 15 to 110 mN/m is also observed during the 24 h period (kinetics not shown), a fact that is consistent with the increase of the surface pressure 6 h after the beginning of the adsorption (Figure 3 insert) and the occurrence of the polyphenol in the adsorption layer (Figure 7). Moreover, the curve of Egc/ $\beta$ -casein shows a plateau of the elastic component around 110 mN/m instead of a maximum (Figure 8). This is in good agreement with its unreduced kinetics even with high bulk concentration of Egc.

On the contrary, the viscous part of the modulus for these three polyphenols is not significant. It remains always lower than 20 mN/m. Compared to the complex dilational modulus of the pure  $\beta$ -casein layer at the concentration used in the same experimental conditions (frequency of 0.1 Hz and surface pressure of  $\sim 19$  mN/m), the elastic part is around 15 mN/m, and the viscous part is negligible as is already observed in the literature (54). It can be clearly seen that the elastic component of the dilational behavior of  $\beta$ -casein is more affected by the presence of galloylated polyphenols or by that with a triphenol group rather than the viscous part. No effect was noticed on moduli with the other polyphenols, Ec, C, or G.

To conclude this part on the rheology of  $\beta$ -casein/ $\phi$  layers, it can be stated that the behavior of layers formed of polyphenol/protein mixtures is rather complex. The increases in polyphenol and protein surface concentrations and in the dilational modulus with incubation time are related to the nature and the structure of the polyphenol. Moreover, in the adsorption layers, only the polyphenols with a triphenol group, that are also the most sensitive to oxidation, induce such variations of modulus. In this respect, it is noteworthy that autoxidation of polyphenols can occur under our operating conditions (high pH, air/liquid interface, and room temperature) (55), yielding various oligomeric products (56) that are likely to interact more readily with  $\beta$ -casein than their monomeric precursor. Moreover, the continuous and relatively slow increase of the modulus is consistent with the oxidation rate reported for EgCG under similar conditions. For example, the extent of oxidation of EgCG in a 1 g/L solution is 50% after 5 h at pH 7, 30 °C with 2.5 mg/L

**Table 1.** Effect of Phenols on the Optical Parameters of the  $\beta$ -Casein Adsorption Layers<sup>a</sup>

$\phi$	$C_{\text{bulk}}$ (mg/L)	$-\bar{\rho}_B$	$n_{589\text{nm}}$	$k_{280}$	$h$ (Å)	$\chi^2$	$\Gamma_{\phi}$ (mg/m <sup>2</sup> )	$\Gamma_{\text{cas}}$ (mg/m <sup>2</sup> )	$\Gamma_{\text{tot}}$ (mg/m <sup>2</sup> )	$R_{\text{layer}}$
		0.011	1.420 ( $\pm 0.032$ )	$\emptyset$	60	0.0041		2.85 ( $\pm 1.10$ )	2.85 ( $\pm 1.10$ )	
EgcG	37	0.020	1.460 ( $\pm 0.029$ )	0.020 ( $\pm 0.001$ )	60	0.0070	0.91 ( $\pm 0.05$ )	3.22 ( $\pm 0.92$ )	4.13 ( $\pm 0.96$ )	15 ( $\pm 3$ )
EcG	30	0.017	1.449 ( $\pm 0.022$ )	0.011 ( $\pm 0.001$ )	60	0.0051	0.43 ( $\pm 0.04$ )	3.36 ( $\pm 0.69$ )	3.79 ( $\pm 0.73$ )	17 ( $\pm 1$ )
Egc	100	0.019	1.454 ( $\pm 0.023$ )	0.006 ( $\pm 0.002$ )	60	0.0047	2.00 ( $\pm 0.67$ )	1.87 ( $\pm 0.06$ )	3.87 ( $\pm 0.73$ )	85 ( $\pm 25$ )
Ec	100	0.011	1.417 ( $\pm 0.015$ )	$\emptyset$	60	0.0080		3.08 ( $\pm 0.50$ )	3.08 ( $\pm 0.50$ )	
C	100	0.011	1.413 ( $\pm 0.021$ )	$\emptyset$	60	0.0025		1.99 ( $\pm 0.70$ )	1.99 ( $\pm 0.70$ )	
gallic acid	100	0.010	1.409 ( $\pm 0.026$ )	$\emptyset$	60	0.0050		2.51 ( $\pm 0.87$ )	2.51 ( $\pm 0.87$ )	

<sup>a</sup> All measurements were performed at quasi-equilibrium (24 h adsorption). The concentration of  $\beta$ -casein in the bulk was 0.42  $\mu\text{M}$  in Mops buffer (10 mM, pH 7). The optical parameters were calculated using a one-layer model with a thickness of 60 Å and minimizing the  $\chi^2$  between the experimental and the calculated values. The real part of the refractive index,  $n$ , was calculated using a dispersion law in the visible wavelength range. The imaginary part of the refractive index,  $k$ , was calculated at 280 nm  $\pm 1$  nm using a numerical inversion of the Drude equation. The surface concentrations ( $\Gamma$ ) of each component were calculated as described in previous studies (29, 44).  $R_{\text{layer}}$  is the molar ratio  $\phi/\beta$ -cas in the adsorption layer. ( $\emptyset$ ) undetectable.

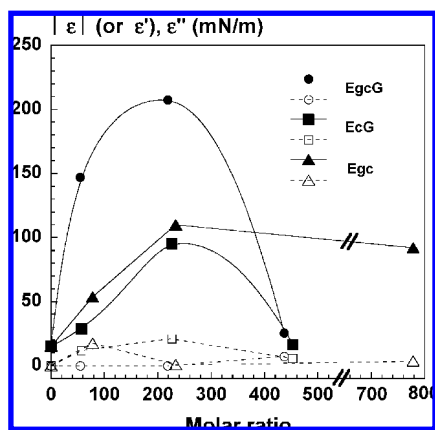


**Figure 8.** Effect of the bulk concentration of phenolic compounds on the complex dilational modulus ( $|\epsilon|$ ), the elastic ( $\epsilon'$ , closed symbols), and the viscous ( $\epsilon''$ , open symbols) parts of the dilational modulus of the  $\beta$ -casein adsorption layer at quasi-equilibrium state ( $\approx 24$  h) with EgcG, EcG, and Egc.  $\beta$ -Casein (10 mg/L) in Mops buffer at pH 7. In these conditions,  $|\epsilon|$  is similar to the elastic part,  $\epsilon'$ .

oxygen (55). Finally, the addition of an antioxidant such as DTT impedes the modulus increase, whereas it does not modify the adsorption behavior of pure  $\beta$ -casein solutions (29), confirming the role of polyphenol oxidation in the observed changes.

In conclusion of this part on the formation of  $\beta$ -casein/polyphenol adsorption layers, it can be rationalized that (1) the three polyphenols with a triphenol feature, EgcG, EcG, and Egc are found in the adsorption layer where a slow process of dilational modulus increase is also noticed. This process seems to be linked to the oxidation of the phenolics. (2) Only EgcG and EcG, with a galloyl substituent on C3, lower the  $\beta$ -casein effective concentration, suggesting an aggregation process between the protein and the polyphenol in the bulk, decreasing the diffusion of the protein toward the interface, a process that does not happen with Egc or with the other low molecular mass phenolics.

An important question now is the status of association between molecules in the bulk and its consistency, or not, with the status deduced from the surface studies.

**Complex Formation in the Bulk.** Complex formation was checked by dynamic light scattering to detect large structures and by ESI-MS to analyze the actual chemical composition of the complexes. In that case, special attention was paid to the effect of oxidation.

**Dynamic Light Scattering.** The bulk concentration of casein was 50 mg/L, which is far below the critical micellar concentration ( $\approx 1$  g/L) and five times larger than that for surface property measurements. This casein bulk concentration is large enough

**Table 2.** Scattering Intensities ( $I$ ) and Hydrodynamic Radii of Particles ( $R_h$ ) in EgcG- $\beta$ -Casein Mixtures<sup>a</sup>

molar ratio (EgcG/ $\beta$ -casein)	$C_{\text{EgcG}}$ (g/L)	$I_{(0h)}$ (a.u.)	$R_{h(0h)}$ (nm)	$I_{(24h)}$ (a.u.)	$R_{h(24h)}$ (nm)
$\infty$	0.2	4	59	3	46
$\infty$	0.5	6	44	4	42
0	0	3	16	3	16
520	0.5	210	50	205	54

<sup>a</sup> The bulk protein concentration is 2.1  $\mu\text{M}$  in MOPS buffer (10 mM, pH 7). Light scattering measurements were carried out 0 and 24 h after the mixing of components.

for the sensitivity of the method and is low enough to allow molar ratios with polyphenols similar to those of the surface measurements (Figure 2). In the semilogarithmic scale, the correlation function  $g_1(t)$  of pure casein and pure polyphenol solutions are linear, a result consistent with the idea that all micelles of casein and particles of polyphenol in pure solution are relatively monodisperse. On the contrary, the mixtures EgcG- $\beta$ -casein deviate appreciably from this exponential behavior. Thus, the formed particles are inhomogeneous in size. In the case of pure casein solution, the hydrodynamic radius of the protein is around 16 nm at ambient temperature (Table 2). It was slightly larger than the gyration radius (7 nm) previously determined by small-angle neutron scattering in unfolded buffer conditions, at 4 °C (57). Thus, one can at most suppose that some micelles of  $\beta$ -casein are present in the solution at ambient temperature without denaturant. In the case of pure EgcG solution, the hydrodynamic radii of particles are in the range 40 to 50 nm (Table 2). In the case of EgcG- $\beta$ -casein mixtures, the size of the particles was estimated between 50 and 54 nm with the polyphenol concentration of 0.5 g/L. In all cases, it was constant during 24 h. However, the presence of these particles could be neglected thereafter in comparison with the scattering intensities of the mixtures that increase 40 times (Table 2). As the exponential equation [eq 7] does not apply perfectly, this increase of the scattering intensity can be due to an increase of the number of particles in the bulk or to an increase of the size of the particles. As usual with scattering measurements, the occurrence of soluble EgcG- $\beta$ -casein aggregates is strongly supported by experimental data, but this aggregation could relate to only a small fraction of the casein in solution. Nevertheless, in the same conditions, the ratio of effective to total casein concentration ( $C_{\text{eff}}/C_{\text{tot}}$ ) is near zero (Figure 4). These results support the idea that the formation of these colloidal particles is responsible for the increase in the induction time of the adsorption kinetics of  $\beta$ -casein in the presence of EgcG. However, the increase of the induction time is of the order of 50 ( $\phi/\beta$ -casein increasing from 0 to 520), a value which does not seem realistic for  $R_g$  (29). Thus, the  $R_h$

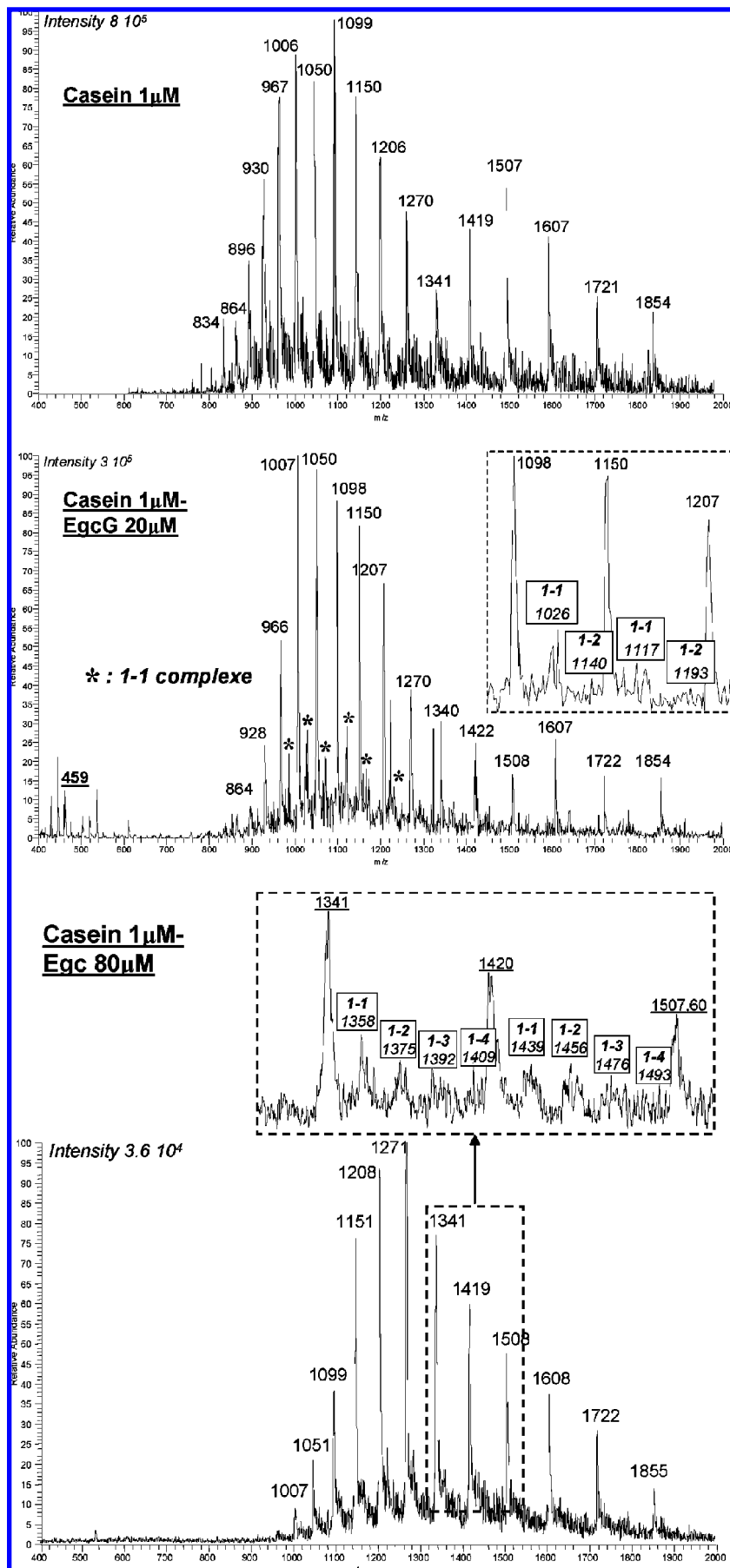


Figure 9. Electrospray mass spectrum of 1  $\mu$ M  $\beta$ -casein solution (a), EgcG/ $\beta$ -casein mixtures at molar ratios of 20 (b), and Egc/ $\beta$ -casein mixtures at a molar ratio of 80 (c) in acetate buffer at pH 7.



**Table 3.** Charge State and Mass/Charge Ratio ( $m/z$ ) of  $\beta$ -Casein, EgcG- $\beta$ -Casein, and Egc- $\beta$ -Casein Mixtures in Acetate Buffer (10 mM, pH 7)<sup>a</sup>

Z $m/z$	26+	25+	24+	23+	22+	21+	20+	19+	18+	17+	16+	15+	14+	13+
$\beta$ -casein	930	967	1005	1050	1097	1151	1206	1271	1341	1420	1508	1608	1723	1854
	EgcG/ $\beta$ -Casein <sup>b</sup>													
1-1		985	1026	1069	1119	1171	1230	1295	1365	1446				
2-1		1002	1044		1140	1193								
	Egc/ $\beta$ -Casein <sup>c</sup>													
1-1			1018	1064	1113	1165	1223	1288	1358	1439	1529	1629		
2-1					1128	1182	1238	1306	1375	1456				
3-1							1254	1322	1392	1476				
4-1									1409	1493				

<sup>a</sup> The  $\beta$ -casein molar concentration in solutions is 1.17  $\mu$ M. <sup>b</sup> Molar ratio EgcG/ $\beta$ -casein range in the bulk from 20 to 60. <sup>c</sup> Molar ratio Egc/ $\beta$ -casein range in the bulk from 34 to 128.

**Table 4.** Summary of the Relationship between the Structure of the Polyphenol and Their Effects on Surface and Bulk Properties of  $\beta$ -Casein

	kinetics	structure	dilational modulus	complexes in the bulk
EgcG	+	+	+	+
EcG	+	+	+	not studied
Egc	-/+	+	+	+
Ec	-	-	-	-
C	-	-	-	not studied
gallic acid	-	-	-	not studied

increase linked to the scattering intensity increase does not completely explain this increase induction time, which may also be affected by a decrease of the hydrophobicity of the polypeptide chain and a more compact structure due to the formation of bonds between the polyphenol and the polypeptide chain. Experimentally, the induction time measured with EcG is significantly larger than with EgcG (**Figure 4**), a fact consistent with the formation of more hydrophobic interactions between the former and  $\beta$ -casein as previously indicated by their values of the partition coefficient of 26.5 and 9.1 in octan-1-ol/water, respectively (48).

**Electrospray Ionization Mass Spectrometry. Complex Analysis.** The electrospray mass spectrum of pure  $\beta$ -casein solution is presented in **Figure 9a**. Each peak corresponds to a different charge state of the protein, as electrospray ionization sources generate multicharged ions (**Table 3**). The first observation is that the measured intensities in the positive ion mode are quite higher than those measured in the negative ion mode. Since, at pH 7,  $\beta$ -casein is charged negatively ( $pI \approx 5.5$ ), the charge state of the protein is modified during electro-nebulization. All charge states between  $13^+$  and  $30^+$  are observed. The measured  $m/z$  values are slightly higher than those calculated from the protein mass (24089 g/mol) (two to three more units). This weak shift indicates that the positive charge of  $\beta$ -casein does not come only from protons ( $H^+$ ) but also from the complexation of some ammonium ions ( $NH_4^+$ ) on the protein, which increases the  $m/z$  values.

Polyphenol/protein complexes in solution were detected by ESI-MS at EgcG/ $\beta$ -casein molar ratios of 20, 40, and 60 with a bulk protein concentration of 1.17  $\mu$ M (28 mg/L) immediately after mixing protein and  $\phi I$  (**Figure 9b**). The intensities of the peaks corresponding to the various charge states of the protein are much lower in the presence of EgcG, meaning that a large fraction of the protein cannot be observed any more by mass spectrometry. This may be due to ion suppression effect or to involvement of the protein in molecular complexes with EgcG, as indicated by measurements of surface properties, although the molar ratio was somewhat lower for the MS experiments. The intensity of the EgcG signal detected at  $m/z = 459$  increased with its concentration, suggesting that some of it was present

in the free state. Closer examination of the mass data shows the presence of additional peaks, corresponding to EgcG/ $\beta$ -casein 1-1 and 2-1 complexes (**Table 3**), between the protein signals, confirming the hypothesis of complex formation. Complexes of higher stoichiometry may also be present but not detected due to overlapping with other mass signals or to a low signal intensity compared to the background noise. It is also possible that the EgcG/ $\beta$ -casein complexes of superior order, corresponding to the aggregates evidenced by light scattering, do not enter in the mass range of measurement of the mass spectrometer because of their lower charge state and thus higher  $m/z$  value. This may explain the discrepancy between the stoichiometries of the observed complexes and the molar ratios of five determined by ellipsometry in the adsorption layer formed from EgcG/ $\beta$ -casein mixtures after 1 h of adsorption (29) or of 15 after 24 h. Thus, formation of particles or aggregation of EgcG/ $\beta$ -casein complexes as reported at a molar ratio above 10 may be responsible for the poor response of  $\beta$ -casein and of EgcG/ $\beta$ -casein complexes in ESI-MS (58).

In the case of Egc-casein mixtures, the intensities of the  $\beta$ -casein peaks are of the same order of magnitude as in the  $\beta$ -casein pure solution (**Figure 9c**). In contrast, the free Egc signal was not detected when it was in mixture with the protein. This suggests that all Egc molecules were involved in complexes with  $\beta$ -casein or that in this case competition for charge in the mass source was in favor of  $\beta$ -casein. Moreover, Egc/ $\beta$ -casein complexes of 1-1, 2-1, 3-1, and 4-1 stoichiometries were detected by mass spectrometry in all solutions with bulk molar ratios between 34 and 128 (**Figure 9c**) as compared to  $85 \pm 25$  obtained by ellipsometry after 24 h of adsorption. Although Egc- $\beta$ -casein complexes may have formed during transfer to the interface, this suggests, on one hand, that Egc interacts with  $\beta$ -casein in the bulk phase, and on the other hand, that these complexes remain rather small and do not lead to further aggregation unlike those formed with EgcG. Aggregates have similarly been observed by dynamic light scattering in solutions containing poly-L-proline with EgcG but not with Egc (48). This may also explain why Egc and EgcG affect the adsorption kinetics and properties of the adsorption layer in different ways. In the case of Ec/ $\beta$ -casein mixtures, the electrospray mass spectrum did not reveal any complex, in agreement with the lack of effect of epicatechin on adsorption processes. Interactions of  $\beta$ -casein with the other two phenolic compounds, namely, catechin and gallic acid, were not analyzed by mass spectrometry since, like epicatechin, they were not reported to form complexes with protein, and they do not have any effect on adsorption.

Thus, ESI-MS analyses of polyphenol- $\beta$ -casein mixtures indicate that, among the three compounds tested, Ec does not interact with the protein, whereas Egc and EgcG both interact with it, but in different ways. On the basis of the mass spectra,

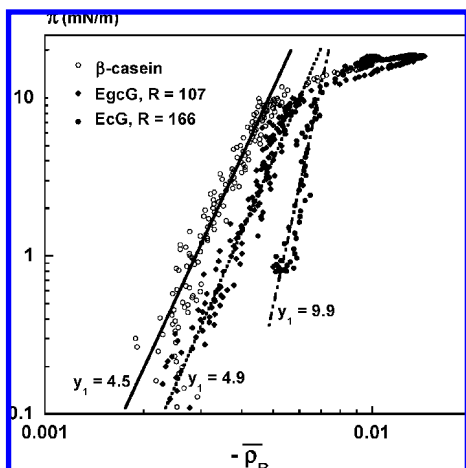


**Figure 10.** Log–log plot of surface pressure  $\pi$  as a function of Brewster ellipticity ( $-\bar{\rho}_B$ ) for pure  $\beta$ -casein and its mixture with EgcG and EcG.  $y_1$  is the slope of the  $\log(\pi)/\log(-\bar{\rho}_B)$  plot calculated according to the equation of state approach (41, 64).

Egc forms low stoichiometry complexes with  $\beta$ -casein with hardly any change in its charge state and no further aggregation. In contrast, complexes between EgcG and  $\beta$ -casein are readily formed but poorly detected. The observed loss of the mass signal intensity is presumably due to the large molecular weight and/or high polydispersity of these complexes as suspected from dynamic light scattering data. This may be related to aggregation of EgcG coated proteins that has been reported at molar ratios above 10 (**Figure 2**) (58).

**Oxidation Status of Polyphenols during the Experiments.** Monitoring of the EgcG solution by electrospray ionization mass spectrometry (ESI-MS) confirmed that it gradually autoxidized under our experimental conditions. Signals that can be attributed to the major known autoxidation dimers (theasinensins at  $m/z = 915$  ( $[M + H]^+$ ),  $m/z = 932$  ( $M + NH_4^+$ );  $m/z = 885$  ( $[M + H]^+$ ),  $m/z = 902$  ( $M + NH_4^+$ ) (56) were detected in the mass spectrum after 6 h of incubation and accumulated thereafter while those of EgcG decayed. Flavanol oxidation products are larger molecular weight species that show increased affinity for proteins compared to their monomeric precursors (59). Besides, oxidation may result in the formation of covalent bonds of the flavanol with the protein (60), which may also explain the modulus increase over time.

It can be concluded, from interfacial and bulk approaches, that the presence of polyphenol/casein complexes in the bulk is always related to the demonstration of the effect of the phenolic compound on the properties of the adsorption layer.

## DISCUSSION

The focus is now on the molecular mechanisms of formation of the complexes, then on the surface properties of the complexes, and finally on the methods developed in this study to investigate the formation of macromolecule–polyphenol complexes.

**Mechanisms of Formation of the Complexes.** The results obtained so far indicate that EgcG, EcG, and Egc form complexes with  $\beta$ -casein, while C, Ec, and G do not. Only the former are discussed here. The first point is the effect of phenol oxidation on the formation of complexes and then of the polyphenol structure required for the complex formation. A treatment of the data in the frame of the multiblock theory (state

equation) was proposed to get some complementary informations on the structure of the layer and on the conformation of the complexes in the adsorption layer.

**Native or Oxidized Phenolics.** Nonoxidized Egc forms complexes with  $\beta$ -casein since 1–1, 2–1, 3–1, and 4–1 stoichiometries were detected by ESI-MS immediately after preparing the solution. However, the occurrence of these polyphenols in the adsorption layer are obvious only after several hours, a fact clearly in favor of a strong interaction of  $\beta$ -casein with the oxidation products. In the case of pure EgcG solution, dimeric oxidation products have been detected in the bulk by mass spectrometry within a few hours of incubation under our experimental conditions. However, ESI-MS cannot distinguish EcG (or EgcG) from their oxidation products in the complexes with stoichiometries higher than 1–1. The difference in mass is too small in front of the number of charge of the complexes. Moreover, the kinetics of the rheological properties of the EgcG and EcG complexes, which are attributed to the interaction with oxidized products have characteristic times that are of the order of 3–5 h (kinetics not shown), while they are of 0.5 h for the adsorption process (EgcG/ $\beta$ -casein  $\approx$  200–250). The data obtained in the conditions of this work support the idea that polyphenols are significantly oxidized after 1 or 2 h. All the processes occurring within shorter time courses should primarily concern the native structure of the polyphenols, while at longer times, oxidation products should also be largely involved. The fact that only the largest phenolics of this work exhibit phenomena, which are attributed to their oxidation could be related to the presence of the triphenol group in the present study (**Figure 1**). Then, the low reduction potentials of their radicals should result in their rapid oxidation in aerated aqueous media (the electrochemical redox potential of EgcG and Egc is 400 mV at pH 7) (61, 62).

**Structure of the Polyphenol.** All the results on the relationship between the structure of the polyphenols and their effects on  $\beta$ -casein adsorption and complex formation in the bulk are summarized in **Table 4**. As explained in the Results section, the molar ratio may be 10 to 20 times larger for measurements of surface properties than for bulk measurements (**Figure 2**); this should not substantially modify their comparison. Particular features seem essential in the observed flavanol–protein interaction: the presence of a galloyl group and either a large enough molecular mass or some other phenolic -OH. The slowdown effect on surface tension kinetics appears only with EgcG and EcG, which have the highest molecular mass and a galloyl group. In fact, the particular behavior of galloylated flavanol monomers has been attributed to their capacity to act as multidentate ligands and to form bridges between polyphenol coated proteins, in the same way as tannin oligomers and polymers (16, 48). The presence of three adjacent hydroxyl groups on the B-ring also seems to play a part in the interactions between flavanols and casein, but in a different way, as evidenced by the comparison between Egc and Ec. The ESI-MS data indicate that Egc forms complexes with  $\beta$ -casein in the bulk phase. Since the presence of an additional hydroxyl renders Egc less hydrophobic than Ec that failed to interact with  $\beta$ -casein, this suggests that hydrogen bonds rather than hydrophobic interactions are involved in the process.

**Some Hypotheses on the Structure of the Complexes in the Surface Layer.** The surface properties measured in this work may be analyzed in terms of the state equation of the protein in the 2-D adsorption layers at the beginning of their formation. Using the scaling law approach of polymers, the thermodynamic model from the state equation (eq 9) may

provide some information on the structure of the layer and on the conformation of the adsorbed macromolecules (63).

$$\pi \cong \Gamma^y \quad (9)$$

where  $\Gamma$  is the surface concentration, and  $y$  is an exponent characteristics of the regime of the interface. It is calculated by combining data obtained as in **Figures 3** and **5** since  $\bar{\rho}_B$  and  $\Gamma$  are proportional to each other (**Figure 10**). The interest of this approach is focused on linear parts of the log–log display (41). The slope  $y_1$  measured at a surface pressure  $<10$  mN/m is directly linked to the fractal dimension of the adsorbed macromolecule at the beginning of the first semidilute regime of the layer (64). In the case of EgcG, the slope ( $y_1 = 4.9$ ), is probably not significantly different from the slope measured for  $\beta$ -casein (4.5) in this study or previous studies (41). On the contrary, in the case of EcG, the slope is close to 9.9, indicating a 2-D structure more collapsed than in the  $\theta$  conditions. It is observed that at the same surface pressure, the ellipticity is larger when a polyphenol occurs in solution, and in the adsorption layer, as expected from **Figure 5** and **Table 1**. A consistent interpretation of these data is that EgcG, which is more hydrophilic than EcG, interacts preferentially with the hydrophilic loops of  $\beta$ -casein (no effect on the  $y$  exponents of the state equation) and does not, in any case, reticulate the polypeptide chains of the hydrophobic (2-D) loops. On the contrary, EcG, with one less OH on the B ring, is more hydrophobic and is located in the vicinity of the hydrophobic loops of the protein, inducing a networking of the 2-D hydrophobic loops. This results in a more collapsed structure of the 2-D loops and a larger  $y_1$  exponent. These probable differences in the mechanism of interaction between  $\beta$ -casein and the two galloylated polyphenols should also have consequences in the structures formed in the bulk phase between  $\beta$ -casein and the different polyphenols. However, no evidence for these differences in the bulk is presently available. The high fractal dimension of the complexes formed with EcG should have consequences on the reactivity and on the properties of their adsorption layer. This is probably the reason for the important differences between the properties of the complexes formed by either EgcG or EcG (**Figure 8**).

Finally, the coordinated bulk and surface analysis of protein–polyphenol interactions provide consistent and complementary information on the structure and on the properties of the complexes. This integrated approach should probably be used as a basic methodology in the future. Besides, the congruence between data obtained by ESI-MS, by DLS, and by surface techniques confirms the relevance of each approach to study polyphenol–protein interactions. The same experimental approach can thus be applied to other proteins such as salivary proteins, which, like  $\beta$ -casein, are random coil polymers with high levels of proline, for prediction of astringency.

#### ACKNOWLEDGMENT

We thank Dr. Michel Delsanti for his help in dynamic light scattering measurements and data analysis. Related discussions with M. Valade and B. Robillard are acknowledged.

#### LITERATURE CITED

- White, T. Tannins—their occurrence and significance. *J. Sci. Food Agric.* **1957**, *8*, 377–385.
- Roberts, E. A. H. The phenolic substances of manufactured tea. VI. The preparation of theaflavin and of theaflavin gallate. *J. Sci. Food Agric.* **1959**, *10*, 176–179.
- Haslam, E. Polyphenol–protein interactions. *Biochem. J.* **1974**, *139*, 285–288.
- Haslam, E. Polyphenol Complexation. In *Polyphenolic Phenomena*; Scalbert, A., Ed.; Paris, 1993; pp 23–39.
- Asano, K.; Shinagawa, K.; Hashimoto, N. Characterization of haze-forming proteins of beer and their roles in chill haze formation. *Am. Soc. Brewing Chemists* **1982**, *40*, 147–154.
- Siebert, K. J.; Troukhanova, N. V.; Lynn, P. Y. Nature of polyphenol–protein interactions. *J. Agric. Food Chem.* **1996**, *44*, 80–85.
- O’Connell, J. E.; Fox, P. D.; Tan-Kintia, R.; Fox, P. F. Effects of tea, coffee and cocoa extracts on the colloidal stability of milk and concentrated milk. *Int. Dairy J.* **1998**, *8*, 689–693.
- O’Connell, J. E.; Fox, P. F. Proposed mechanism for the effect of polyphenols on the heat stability of milk. *Int. Dairy J.* **1999**, *9*, 523–536.
- Bate-Smith, E. C. Astringency in foods. *Food* **1954**, *23*, 124–127.
- Bate-Smith, E. C. Haemalysis of tannins: the concept of relative astringency. *Phytochemistry* **1973**, *12*, 907–912.
- Ozawa, T.; Lilley, T. H.; Haslam, E. Polyphenol interactions: astringency and the loss of astringency in ripening fruit. *Phytochemistry* **1987**, *26*, 2937–2942.
- Kielhorn, S.; J. H. T. Oral sensation associated with the flavan-3-ols (+)-catechin and (-)-epicatechin. *Food Qual. Preference* **1999**, *10*, 109–116.
- Artz, W. E.; Bishop, P. D.; Dunker, A. K.; Schanus, E. G.; Swanson, B. G. Interaction of synthetic proanthocyanidin dimer and trimer with bovine serum albumin and purified bean globulin fraction G-1. *J. Agric. Food Chem.* **1987**, *35*, 417–421.
- Freitas, V. d.; Mateus, N. Structural features of procyanidin interactions with salivary proteins. *J. Agric. Food Chem.* **2001**, *49*, 940–945.
- Haslam, E.; H. Lilley, T.; Warminski, E.; Liao, H.; Cai, Y.; Martin, R.; H. Gaffney, S.; N. Goulding, P.; Luck, G. Polyphenol Complexation, a Study in Molecular Recognition. In *Phenolic Compounds in Food and Their Effect on Health*; 1992; pp 8–50.
- McManus, J. P.; Davis, K. G.; Beart, J. E.; Gaffney, S. H.; Lilley, T. H.; Haslam, E. Polyphenol interactions; some observations on the reversible complexation of polyphenols with proteins and polysaccharides. *J. Chem. Soc., Perkin Trans. 2* **1985**, 1429–1438.
- Baxter, N. J.; Lilley, T. H.; Haslam, E.; Williamson, M. P. Multiple interactions between polyphenols and a salivary proline-rich protein repeat result in complexation and precipitation. *Biochemistry* **1997**, *36*, 5566–5577.
- Bacon, J. R.; Rhodes, M. J. C. Development of a competition assay for the evaluation of the binding of human parotid salivary proteins to dietary complex polyphenols and tannins using a peroxidase-labeled tannin. *J. Agric. Food Chem.* **1998**, *46*, 5083–5088.
- Sarni-Manchado, P.; Cheynier, V. Study of non-covalent complexation between catechin derivatives and peptides by electrospray ionisation mass spectrometry. *J. Mass Spectrom.* **2002**, *37*, 609–616.
- Vidal, S.; Francis, L.; Guyot, S.; Marnet, N.; Kwiatkowski, M.; Gawel, R.; Cheynier, V.; Waters, E. J. The mouth-feel properties of grape and apple proanthocyanidins in a wine-like medium. *J. Sci. Food Agric.* **2003**, *83*, 564–573.
- Murray, N. J.; Williamson, M. P.; Lilley, T. H.; Haslam, E. Study of the interaction between salivary proline-rich proteins and a polyphenol by H-NMR spectroscopy. *Eur. J. Biochem.* **1994**, *219*, 923–935.
- Charlton, A. J.; Baxter, N. J.; Lilley, T. H.; Haslam, E.; McDonald, C. J.; Williamson, M. P. Tannin interactions with a full-length human salivary proline-rich protein display a stronger affinity than with single proline-rich repeats. *FEBS Lett.* **1996**, *382*, 289–292.
- Tomba, P. Intrinsically unstructured proteins evolve by repeat expansion. *BioEssays* **2003**, *25*, 847–855.
- Hagerman, A. E. *Chem. Signif. Condens. Tannins*, [Proc. North Am. Tannin Conf.], 1st ed., pp 323–333.
- Swaigood, H. E. *Development in Dairy Chemistry*; Applied Science Publishers: London, 1982; pp 1–59.
- Chamkha, M.; Cathala, B.; Cheynier, V.; Douillard, R. Phenolic composition of champagnes from Chardonnay and Pinot Noir vintages. *J. Agric. Food Chem.* **2003**, *51*, 3179–3184.

- (27) Péron, N.; Cagna, A.; Valade, M.; Bliard, C.; Aguié-Béghin, V.; Douillard, R. Layers of macromolecules at the champagne/air interface and the stability of champagne bubbles. *Langmuir* **2001**, *17*, 791–797.
- (28) Abou Saleh, K.; Aguié-Béghin, V.; Foulon, L.; Valade, M.; Douillard, R. Characterization by optical measurements of the effects of some stages of champagne technology on the adsorption layer formed at the gas/wine interface. *Langmuir* **2007**, *23*, 7200–7208.
- (29) Sausse, P.; Aguié-Béghin, V.; Douillard, R. Effects of epigallocatechin gallate on beta-casein adsorption at the air/water interface. *Langmuir* **2003**, *19*, 737–743.
- (30) Borch, J.; Jorgensen, T. J. D.; Roepstorff, P. Mass spectrometric analysis of protein interactions. *Curr. Opin. Chem. Biol.* **2005**, *9*, 509–516.
- (31) Pramanik, B. N.; Bartner, P. L.; Mirza, U. A.; Liu, Y.-H.; Ganguly, A. K. Electrospray ionization mass spectrometry for the study of non-covalent complexes: an emerging technology. *J. Mass Spectrom.* **1998**, *33*, 911–920.
- (32) Schwartz, B. L.; Gale, D. C.; Smith, R. D. Noncovalent Interactions Observed Using Electrospray Ionization. In *Methods in Molecular Biology*; Chapman, J. R., Ed.; pp 115–127.
- (33) Vergé, S.; Richard, T.; Moreau, S.; Richelme-David, S.; Vercauteren, J.; Promé, J. C.; Monti, J. P. First observation of non-covalent complexes for a tannin-protein interaction model investigated by electrospray ionisation mass spectroscopy. *Tetrahedron Lett.* **2002**, *43*, 2363–2366.
- (34) Mercier, J. C.; Maubois, J. L.; Poznanski, S.; Ribadeau-Dumas, B. Fractionnement préparatif des caséines de vache et de brebis par chromatographiesur D.E.A.E. cellulose, en milieu urée et 2-mercaptoéthanol. *Bull. Soc. Chim. Biol.* **1968**, *50*, 521–530.
- (35) Cagna, A.; Esposito, G.; Rivière, C.; Housset, S.; Verger, R. 33rd International Conference on Biochemistry of Lipids, Lyon, France, 1992.
- (36) McLeod, C. A.; Radke, C. J. *J. Colloid Interface Sci.* **1993**, *160*, 435.
- (37) Labourdenne, S.; Gaudry-Rolland, N.; Letellier, S.; Lin, M.; Cagna, A.; Esposito, G.; Verger, R.; Rivière, C. The oil-drop tensiometer: potential applications for studying the kinetics of (phospho)lipase action. *Chem. Phys. Lipids* **1994**, *71*, 163–173.
- (38) Lucassen, J. Dynamic Properties of Free Liquid Films and Foams. Anionic Surfactants-Physical Chemistry of Surfactant Action. In *Surfactant Science Series*; Schick, M. J., Ed.; New York, 1981; pp 217–265.
- (39) Hambardzumyan, A.; Aguié-Béghin, V.; Panaïotov, I.; Douillard, R. Effect of frequency and temperature on rheological properties of beta-casein adsorption layers. *Langmuir* **2003**, *19*, 72–78.
- (40) Benjamins, J.; Cagna, A.; Lucassen-Reynders, E. H. Viscoelastic properties of triacylglycerol/water interfaces covered by proteins. *Colloids Surf.* **1996**, *114*, 245–254.
- (41) Hambardzumyan, A.; Aguié-Béghin, V.; Douillard, R. beta-casein and symmetrical triblock copolymer (PEO-PPO-PEO and PPO-PEO-PPO) surface properties at the air-water interface. *Langmuir* **2004**, *20*, 756–763.
- (42) Drude, P. Reflexion und brechung bei oberflächenschichten. *Ann. Phys. Chem. (Leipzig)* **1891**, *43*, 126–157.
- (43) Azzam, R. M. A.; Bashara, N. M. *Ellipsometry and Polarized Light*; Amsterdam, 1987.
- (44) Aguié-Béghin, V.; Baumberger, S.; Monties, B.; Douillard, R. Formation and characterization of spread ligin layers at the air water interface. *Langmuir* **2002**, *18*, 5190–5196.
- (45) de Freijter, J. A.; Benjamins, J.; Veer, F. A. Ellipsometry as a tool to study the adsorption behavior of synthetic and biopolymers at the air-water interface. *Biopolymers* **1978**, *17*, 1759–1772.
- (46) Puff, N.; Cagna, A.; Aguié-Béghin, V.; Douillard, R. Effect of ethanol on the structure and properties of b-casein adsorption layers at the air-buffer interface. *J. Colloid Interface Sci.* **1998**, *208*, 405–414.
- (47) Chu, B. *Laser Light Scattering: Basic Principles and Practice*, 2nd ed.; Academic Press, Inc.: New York, 1991; p 352.
- (48) Poncet-Legrand, C.; Edelmann, A.; Putaux, J. L.; Cartalade, D.; Sarni-Manchado, P.; Vernhet, A. Poly(-proline) interactions with flavan-3-ols units: Influence of the molecular structure and the polyphenol/protein ratio. *Food Hydrocolloid* **2006**, *20*, 687–697.
- (49) Poncet-Legrand, C.; Gautier, C.; Cheynier, V.; Imberty, A. Interactions between flavan-3-ols and poly(L-proline) studied by isothermal titration calorimetry: Effect of the tannin structure. *J. Agric. Food Chem.* **2007**, *55*, 9235–9240.
- (50) Jöbstl, E.; Howse Jonathan, R.; Fairclough, J. P. A.; Williamson Mike, P. Noncovalent cross-linking of casein by epigallocatechin gallate characterized by single molecule force microscopy. *J. Agric. Food Chem.* **2006**, *54*, 4077–4081.
- (51) Ybert, C.; di Meglio, J. M. Study of protein adsorption by dynamic surface tension measurements: Diffusive regime. *Langmuir* **1998**, *14*, 471–475.
- (52) Brand-Williams, W.; Cuvelier, M. E.; Berset, C. Use of a Free Radical Method to Evaluate Antioxidant Activity. *Lebensm.-Wiss. Technol.* **1995**, *28*, 25–30.
- (53) Monties, B. Potentiel d'oxido-reduction des polyphénols. Caractérisation potentiométrique des constituants phénoliques du jus de pomme et des boissons. *Ann. Technol. agric.* **1967**, *16*, 251–268.
- (54) Maldonado-Valderrama, J.; Fainerman, V. B.; Galvez-Ruiz, M. J.; Martin-Rodriguez, A.; Cabrerizo-Vilchez, M. A.; Miller, R. Dilatational rheology of  $\beta$ -casein adsorbed layers at liquid-fluid interfaces. *J. Phys. Chem. B* **2005**, *109*, 17608–17616.
- (55) Zimeri, J.; Tong, C. H. Degradation kinetics of (-)-epigallocatechin gallate as a function of pH and dissolved oxygen in a liquid model system. *J. Food Sci.* **1999**, *64*, 753–758.
- (56) Sang, S.; Lee, M.-J.; Hou, Z.; Ho, C.-T.; C-S., Y. Stability of tea polyphenol (-)-epigallocatechin-3-gallate and formation of dimers and epimers under common experimental conditions. *J. Agric. Food Chem.* **2005**, *53*, 9478–9484.
- (57) Calmettes, P.; Durand, D.; Smith, J. C.; Desmadril, M.; Minard, P.; Douillard, R. Structure of proteins unfolded by guanidinium chloride. *J. Phys. I* **1993**, *3*, 253–256.
- (58) Jöbstl, E.; O'Connell, J.; Fairclough, J. P. A.; Williamson Mike, P. Molecular model for astringency produced by polyphenol/protein interactions. *Biomacromolecules* **2004**, *5*, 942–949.
- (59) Guyot, S.; Pellerin, P.; Brillouet, J. M.; Moutounet, M.; Cheynier, V. Inhibition of beta-glucosidase (*Amygdalae Dulces*) by (+)-catechin oxidation products and procyanidin dimers. *Biosci. Biotechnol. Biochem.* **1996**, *60*, 1131–1135.
- (60) Haslam, E.; Lilley, T. H. Natural astringency in foodstuffs. A molecular interpretation. *Crit. Rev. Food Sci. Nutr.* **1988**, *27*, 1–40.
- (61) Jovanovic, S. V.; Hara, Y.; Steenzen, S.; Simic, M. G. Antioxidant potential of galliccatechins. A pulse radiolysis and laser photolysis study. *J. Am. Chem. Soc.* **1995**, *117*, 9881–9888.
- (62) Hagerman, A. E.; Dean, R. T.; Davies, M. J. Radical chemistry of epigallocatechin gallate and its relevance to protein damage. *Arch. Biochem. Biophys.* **2003**, *414*, 115–120.
- (63) Aguié-Béghin, V.; Leclerc, E.; Daoud, M.; Douillard, R. Asymmetric multiblock copolymers at the gas-liquid interface: phase diagram and surface pressure. *J. Colloid Interface Sci.* **1999**, *214*, 143–155.
- (64) Douillard, R.; Daoud, M.; Aguié-Béghin, V. Polymer thermodynamics of adsorbed protein layers. *Curr. Opin. Colloid Interface Sci.* **2003**, *8*, 380–386.

Received for review May 30, 2008. Revised manuscript received August 29, 2008. Accepted August 30, 2008. This work was supported by the Région Champagne-Ardenne and the Conseil Général de Reims (France).